Available online at www.sciencedirect.com

ScienceDirect

Energy Procedia 124 (2017) 215–224

Energy Procedia

www.elsevier.com/locate/procedia

7th International Conference on Silicon Photovoltaics, SiliconPV 2017

Modeling of recombination strength at grain boundaries after phosphorus diffusion gettering and the effect of hydrogen passivation

Marie S. Wiig[a], Halvard Haug[a,b], Rune Søndenå[a] and Erik S. Marstein[a,b]

[a]Solar Energy Department, Institute for Energytechnology, Instituttveien 18, 2007 Kjeller, Norway
[b]University of Oslo, Institute for Technology Systems, Pb 70, 2027 Kjeller, Norway

Abstract

We present a method for extracting local recombination rates from photoluminescence images of double side passivated wafers, using simulations of lateral charge carrier diffusion in two dimensions. By fitting the simulated carrier lifetime map with a calibrated photoluminescence image, the recombination profiles in bulk and at grain boundaries (GBs) can be extracted. This method can be used to quantify the GB recombination velocity even if the carrier concentration in bulk is simultaneously affected by recombination at multiple GBs. High performance multicrystalline wafers from a commercially cast ingot with low impurity concentrations were studied. The GBs were completely passivated applying a hydrogenation step simulated contact firing of a hydrogen rich silicon nitride (SiN) film. The bulk carrier recombination profile from simulations of carrier diffusion after phosphorus diffusion gettering is similar to the measured lifetime after phosphorus diffusion gettering and firing. This indicates that the main role of hydrogen passivation is deactivation of the GB recombination. No additional enhancement of the bulk lifetime is observed after hydrogen passivation.

© 2017 The Authors. Published by Elsevier Ltd.
Peer review by the scientific conference committee of SiliconPV 2017 under responsibility of PSE AG.

Keywords: Grain boundary recombination; PL imaging; charge carrier diffuion

1. Introduction

The performance of multicrystalline silicon (mc-Si) solar cells is limited by impurities, crystal defects and interactions thereof [1-3]. Crystal defects such as grain boundaries and dislocations are easily decorated with impurity species, forming recombination active defects in the material [4-6]. Dislocation clusters are especially

1876-6102 © 2017 The Authors. Published by Elsevier Ltd.
Peer review by the scientific conference committee of SiliconPV 2017 under responsibility of PSE AG.
10.1016/j.egypro.2017.09.255

detrimental to the minority carrier lifetime in conventional mc-Si as dislocations multiply and grow during solidification [7-9].

The recent years there has been a shift towards seed assisted growth of mc-Si, so-called high performance mc silicon (HPMC-Si), in the photovoltaic industry. HPMC-Si offers increased control of the grain size and grain orientation reducing dislocation growth, thus increasing the performance of the final solar cells [8, 10]. As a result of the seeding method used during casting grain sizes are smaller in HPMC-Si relative to conventional mc-Si [11, 12]. The high density of grain boundaries (GBs) makes quantifying and understanding recombination properties at these defects increasingly important.

Phosphorus diffusion gettering (PDG) is efficient in removing fast diffusing metallic impurities from the silicon wafer [13, 14]. However, the average effective lifetime has still been observed to decrease in the central region of a silicon block of industrial quality material with initially low impurity levels [9, 15]. This apparent decrease in average lifetime after PDG can be related to strong activation of recombination at the GBs after PDG [16, 17]. With a good surface passivation diffusion of carriers from bulk grains to strongly recombining GBs may affect the steady state carrier concentration in the bulk grains, which never reach a level limited by the bulk lifetime in the grain. This is typical in HPMC-Si with small grain sizes. This steady state carrier concentration can be measured by photoluminescence (PL) imaging. This is a fast contactless technique with high spatial resolution for studying the carrier lifetime in silicon wafers. The PL signal can be calibrated by a quasi-steady state photoconductance (QSSPC) measurement to give a steady state carrier lifetime image at a fixed generation rate.

In order to quantify the recombination at the GBs we calculate the surface recombination velocity of the GB (S_{GB}) defined as a surface recombination velocity at the interface between two grains [18], this describes the intrinsic recombination properties of the GBs independent of measurement conditions or other sample parameters. PL contrast has previously also been used to quantify the recombination strength of GBs, but this technique only give a relative value which cannot be compared to others.

For double side passivated wafers the diffusion affected region around a GB can be several mm, which for small grains implies that the effective lifetime in a grain can be affected by recombination at several GBs. In this case simulation of the recombination profile along one direction will not be sufficient. To avoid influence of nearby GBs the SRV has previously been simulated from single side passivated wafers[18]. However this required modeling of the PL signal rather than only the charge carrier concentration, which requires detailed knowledge of the sensors in the PL setup. Also a separate set of double side passivated samples were required to access the bulk lifetime. To reach an appropriate injection level with infinite rear SRV they used 330 µm rather than more typical 180 µm thick wafers. We will present another approach to access the recombination lifetime in bulk and at GBs from double side passivated wafers, by using 2D simulation of diffusion in the direction of the wafer surface. Simultaneous influence of multiple recombining GBs are then accounted for.

The recombination activity of GBs after PDG is known to be reduced after a subsequent contact firing of a hydrogen rich SiN. How this process influences on bulk and GB recombination has also been studied and correlated to bulk lifetime from the simulations. The material used is commercially cast HPMC-Si.

2. Sample preparation

Neighbouring wafers from the center possition of a block were selected for the experiment. The processing of the wafers were stopped at three different stages of the solar cell process: ungettered, after phosphorus diffusion gettering (PDG) and after PDG and a subseququent hydrogen passivation of the grain boundaries (PDG + firing). A simulated contact firing process with a peak temperature close to 800 ^{o}C with a hydrogen rich ARC/passivation layer present is used for hydrogen passivation of grain boundaries. The process flows for the three neighboring wafers are shown in Fig. 1.

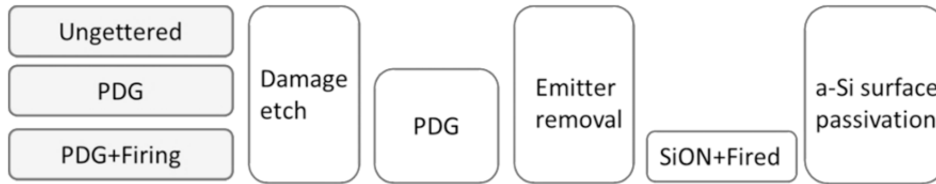

Fig. 1. Sample process flow for wafers at different processing stages. P in-diffusion is performed in a POCl3-tube furnace while the simulated contact firing is performed with a hydrogen rich ARC deposited on both sides. All etching steps are the common for all wafers to maintain similar optical properties and surface passivation.

In order to maintain the same sample thickness and optical properties of the surfaces, all silicon etching steps were the same for all wafers. Before lifetime measurements the surfaces were passivated with 40 nm a-Si:H layers on both sides, processed by plasma enhanced chemical vapor deposition (PECVD).

3. PL imaging

PL images were aquired with a LIS-R1 from BT imaging using a high magnification lens imaging an 2.2 x 2.2 cm^2 area with a resolution of 22 µm/pixel[19]. The PL images were calibrated with QSSPC, using a fixed calibration constant obtained at an area of a wafer with homogeneous lifetime after PDG + firing.

The PL spectrum emitted from a silicon wafer ranges from 900 to 1300 nm[20]. Short wavelength photons have a small absorption depth, and if emitted from the rear of the wafer this part of the spectrum therefore has a large probability of being reabsorbed before reaching the front surface and the detector. However, long wavelength photons emitted from the rear of the wafer may travel a long distance through the silicon before escaping the front surface. This path through the wafer may result in a lateral displacement of the detected PL signal with respect to where it was emitted. The same phenomena also occurs in the detector where short wavelength light is absorbed close to where it enter the CCD chip, while long wavelength light can travel further before it is detected, causing a smearing of the signal. This smearing of the signal both from within the wafer and the CCD chip can be reduced by applying a short pass filter in front of the detector [18, 21]. A 1050 nm short pass filter was placed in front of the camera to reduce lateral dispacement of the PL signal. With such a filter only short wavelength PL emitted close to the surface will reach the detector. The displacement of the detected signal from where it was emitted is then small. The effect of applying a 1050 nm short pass filter in front of the detector is shown in Fig. 2. For a homogeneous region, as shown for the ungettered and PDG + fired sample, the effect is as expected small. However for the PDG sample with large lifetime variations the extremes of the lifetime variations are shaved off: the peaks are smaller and the lifetime at the GB appears higher without filtering. In order to study the recombination properties at strongly recombining GBs, as after PDG, filtering the PL signal is of crucial importance.

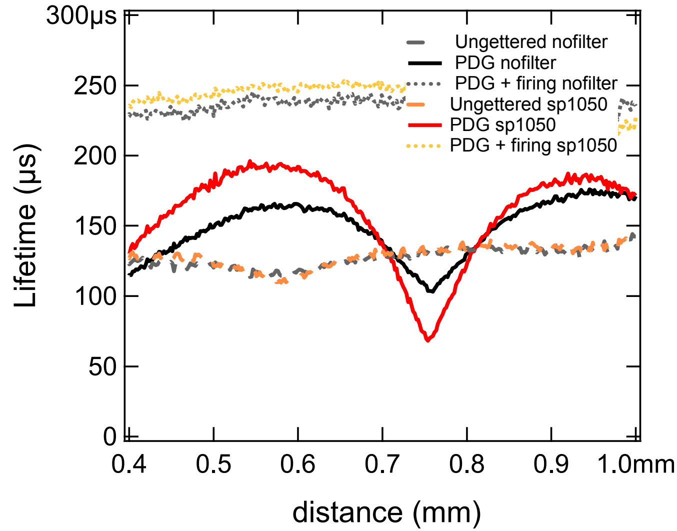

Fig. 2. Calibrated lifetime with and without a 1050 nm short pass filter in front of the detector.

4. Modeling recombination velocity at a GB

The lifetime in a calibrated steady state PL image is directly related to the distribution of carriers through the relation $\tau=\Delta n/G$. Even after filtering the PL signal, the lifetime profiles do not represent the recombination profile in the material itself, but are images of the carrier distribution affected by diffusion of carriers from high to low lifetime regions. The knowledge of carrier diffusion in silicon is in our simulations used to calculate the recombination profile.

The recombination velocity at the GB (S_{GB}) will be calculated form the diffusion profile of carriers from bulk toward the GB. The recombining grain boundary has been defined as a box function; the width of the recombining region is set to 0.1 mm. The lifetime of the two grains separated by the GB is assumed to be homogeneous, but the bulk lifetime of each grain can be set individually. The grain boundary can also be considered as an interface between two neighboring grains and the surface recombination velocity is then defined as the velocity of carriers entering the interface from one side and recombining in the volume of the GB, according to Eq. 1. If the lifetime of the grains on each side of the GB is asymmetric the recombination velocity will also be different, however the recombination velocity has here been defined as the average from both sides. The total surface recombination velocity at the grain boundary (S_{GB}) is determined by the lifetime and the width of the GB.

$$S_{GB} = \frac{1}{2}\int_{x,min\,GB}^{x,max\,GB} \frac{1}{\tau_{R,GB}} dx \tag{1}$$

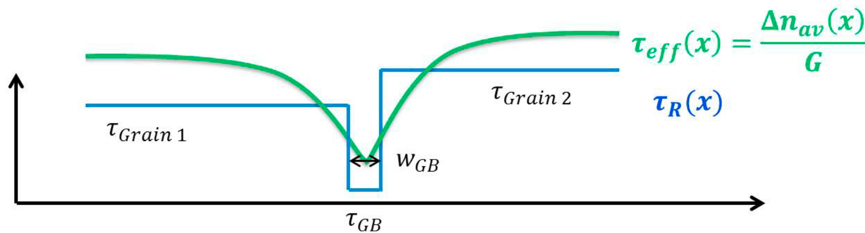

Fig. 3. Schematic of the model used for simulating the recombination velocity at a GB. Showing the recombination profile and corresponding effective lifetime.

The charge carrier concentration is obtained from a steady state photoluminescence image, giving a steady state charge carrier concentration which in 2D can be described by

$$0 = G(x,y) - \frac{n(x,y)}{\tau_R(x,y)} + D\nabla^2 n(x,y). \quad (2)$$

Where G is the generation rate, n is the concentration of electrons and τ_R is the recombination lifetime.

High surface recombination velocity or very low lifetime results in an inhomogeneous charge carrier concentration through the thickness of the wafer resulting in a gradient in y-direction. However for double side passivated wafers with low front and rear surface recombination velocities, this simplifies to a 1D problem, where the carrier concentration only varies in x-direction perpendicular to the direction of the GB. The charge carrier distribution perpendicular to the grain boundary can be found directly from the calibrated PL image, as $\tau_{eff}=\Delta n/G$. The lifetime of the bulk grains and at the GB can be found by fitting the charge carrier profile from the PL image by Eq. 2, where a homogeneous generation rate through the wafer has been assumed. S_{GB} is found by integrating the fitted lifetime profile over the width of the GB, according to Eq (1).

For double side passivated wafers strong recombination at the GB, may conceal the bulk lifetime in small grains. If the effective lifetime in a grain is affected by recombination at several GBs, the above simulation of the recombination profile along x-direction will not be sufficient. However, as described above for a double side passivated sample the carrier profile will be uniform in y-direction (depth). From this the diffusion equation in Eq. 2 can be redefined to describe diffusion along the x and z direction parallel to the wafer surface, while the depth profile is constant. In this 2D simulation τ_R is defined as a function of the position on the surface, rather than a depth profile as in the 1D simulation. A 2D map of the GBs is required as input to the model, this can be measured by electron back-scattering diffraction (EBSD). However, in this case it has simply been drawn from highly recombining GB's appearing in the lifetime image. The width of the GB is then defined by the width drawn in the map. A lifetime is assigned to each grain and to each type of GBs. Fig. 4 a) shows the output image from the simulation after fitting the lifetime parameters the simulated lifetime image is given in b) and the calibrated PL image in c).

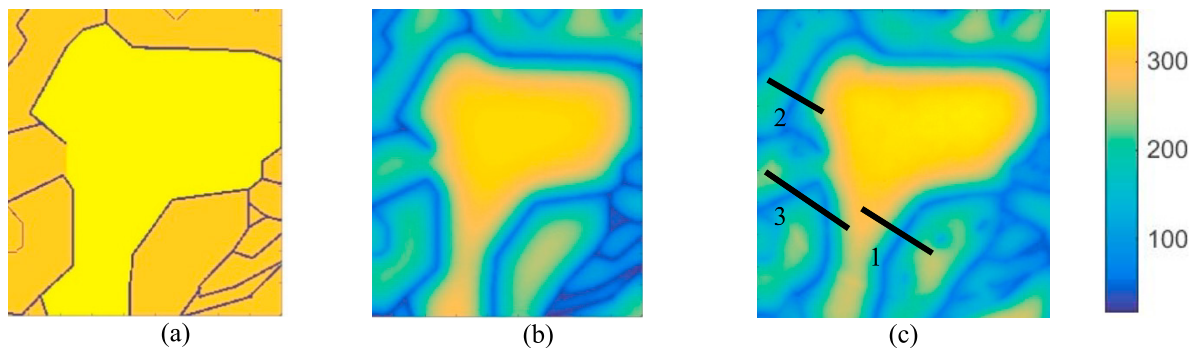

Fig. 4. Output bulk lifetime and GB map, where the GB layout is defined by the input map (a) 2D-simulation of effective lifetime map (b) and PL-image of carrier lifetime (c). The lifetime is given by the color scale.

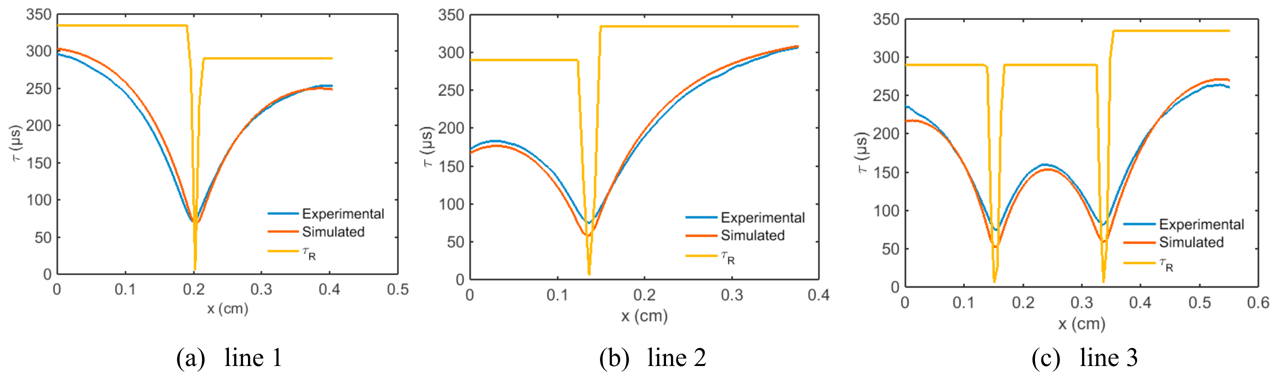

Fig. 5. Line scans comparing experimental and simulated data. Line scans perpendicular to a GB in (a) and (b). At an angle to the GB and simultaneously affected by multiple GBs in (c).

Visually comparing the images in Fig. 4 b) and c), we see that there is a good correspondence between the calibrated PL-image and the simulated lifetime map. In this example, the recombination lifetime of all GBs were set to 5µs, which fits well for most of the GBs, however it overestimates the recombination at the more densely packed GBs at the lower right of the image. When the simulated image fits well with the PL-image, the output GB map gives a good representation of the recombination properties of the wafer after removing the contribution from diffusion, revealing the bulk lifetime of small grains strongly affected by GB recombination. The accuracy of the fit can be further evaluated by comparing selected line scans of the data as shown in Fig. 5. The line scans in Fig. 5 a) and b) shows profiles perpendicular to the GB and at sufficiently large grains to avoid strong influence of other GBs. This is similar to the 1D simulation above. The line scan in Fig. 5 c) shows the lifetime profile crossing two GBs at a slanting angle, and the effective lifetime in the region between in the two GBs are affected by two GBs simultaneously. This lifetime data can only be simulated by the 2D model. The fitted carrier lifetime profiles are shown as yellow lines, labeled τ_R in Fig. 5. As the charge carrier profile is strongly dependent on the bulk lifetime of the grains [18] a fit to the charge carrier profile can give a good estimate for the bulk lifetime. This 2D simulation is an alternative method to using a de-smearing algorithm to find the bulk lifetime [21, 22]. It has the advantage of being intuitively simple and avoiding artefacts which may arise from post-processing of images. However, care must be taken when evaluating the uniqueness of the result and possible correlations between the fitting parameters. The peak effective lifetime from the PL-image of the grain positioned between the two grain boundaries is around 150 µs. After removing the contribution from recombination at the GB to the carrier concentration in bulk, the simulation shows a bulk lifetime of 290 µs. In this case the measured lifetime in the grain measured by PL is dominated by the recombination at the GBs. Comparing the lifetime image in Fig. 4 a) with b) and c), all grains except the big grain in the center is dominated by recombination at the GBs. As the output recombination profile is a result of fitting to a model, the accuracy is somewhat uncertain. For double side passivated wafers a similar model has been shown to be very sensitive to bulk lifetime, while at very high S_{GB} the effective lifetime profile becomes limited by transport of carrier to the GB and S_{GB} saturates[18]. For very high recombination velocities modeling S_{GB} on single side passivated wafers becomes more accurate. Our model does not cover that, as evaluating a non-uniform charge carrier profile depthwise would be required.

5. Injection dependence of S_{GB}

1D simulations of the carrier profile perpendicular to a GB between large grains has been used to calculate the recombination velocity at a GB as a function of injection level. The surface recombination velocity was found to

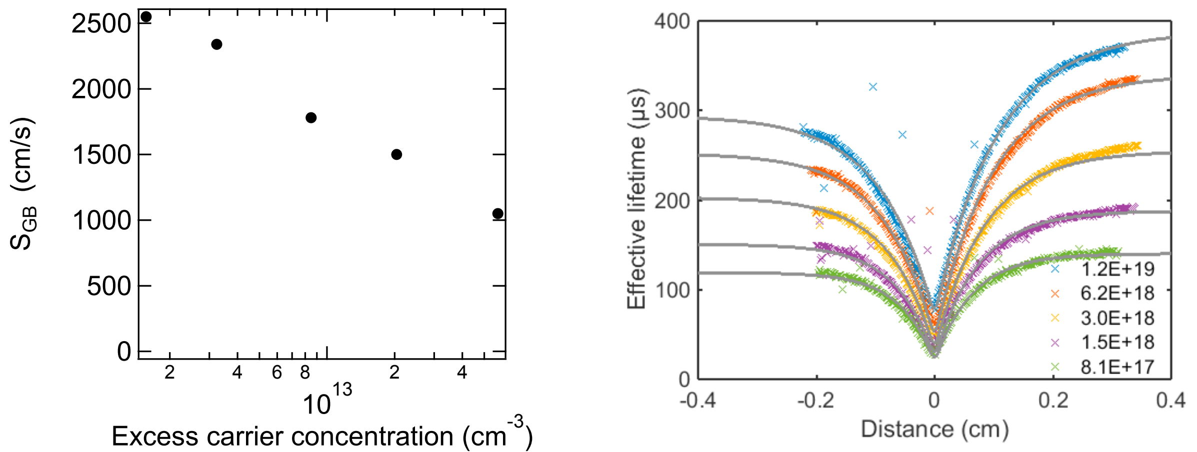

Fig. 6. S_{GB} and lifetime curves at different generation rates, indicated by the color of the data in the figure.

decrease almost linearly with the logarithm of the injection level. The injection level at the GB was calculated from the simulated local recombination lifetime at the given generation rate for the image, assuming a 0.1 mm width of the GB. At low injection the recombination velocity was 2500 cm/s while it decreased to 1000 cm/s at high injection. The calculated recombination velocity of the GB together with the recombination profiles at different generation rate is shown in Fig. 6. To point out the error on the estimated S_{GB} induced by displacement of long wavelength PL, the surface recombination velocity of the same GB was also calculated from an image acquired without a short pass filter, this resulted in almost 3 times lower S_{GB}. S_{GB} was found to be S_{GB} of 1672 cm/s with and 572 cm/s without SP filter at a flux of 0.8e17 cm^{-2}. This emphasizes the importance of having accurate input data in order to extract correct recombination parameters from the carrier diffusion profiles.

6. Hydrogenation passivation of GBs

PL images and recombination profiles have been studied at three different stages of solar cell processing. The lifetime in the ungettered and PDG + firing samples are relatively homogeneous for the imaged region, except for some scattered dislocation clusters. No traces of the GBs can be seen from these two samples, see Fig. 7 .

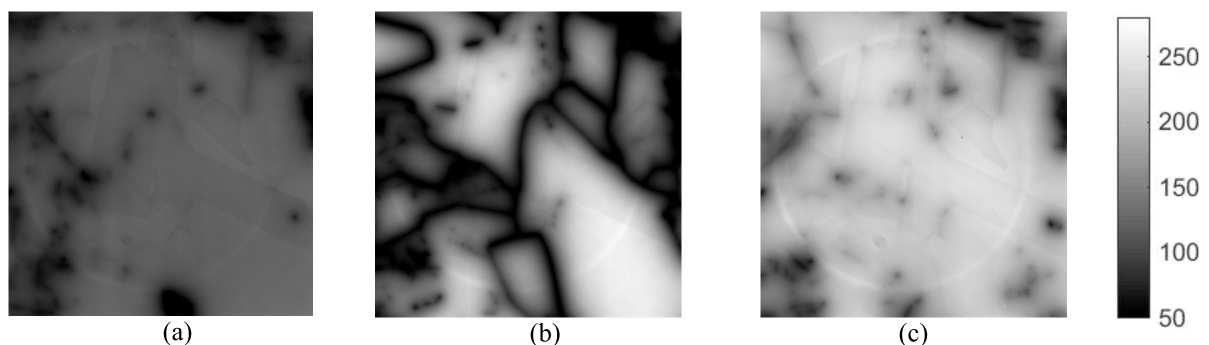

Fig. 7. (a) Ungettered (b) PDG (c) and PDG + firing

The strong recombination appearing at the GBs after PDG is deactivated after firing. The exact mechanism for this is somewhat still unclear, but it has often been referred to as hydrogen passivation. The lifetime after PDG + firing is around 330µs in the best grain compared to below 200 µs before PDG. This means that PDG was efficient in removing lifetime limiting impurities from the bulk. For small grains there is a large increase in lifetime from after PDG to PDG + firing also. However if we compare the bulk lifetime after PDG + firing with τ_R from 2D simulations of GB recombination we observe good correspondence between the fitted bulk lifetime after PDG and the measured bulk lifetime after PDG+H, seen from Fig. 8.

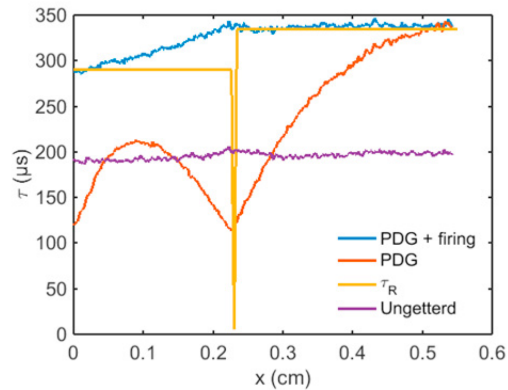

Fig. 8. Carrier lifetime profiles ungetterd purple), PDG red), PDG + firing blue) and simulated yellow).

This indicates that the effect of hydrogen passivation on our samples is only to passivate the GBs. There is no additional gettering effect in bulk, as was recently observed on intentionally contaminated samples after simulated contact firing[23]. This may be due to the low metallic contamination levels after PDG in this wafer, which came from the middle section of an industrially cast ingot of HPMC-Si. To further test if the only effect of firing after PDG is passivation of recombination centers at GBs, the input lifetime map to the 2D simulations, were replaced by a PL-image after PDG + firing where the GBs from the theoretical map were projected on top of the PL image and used as an fixed input instead of as a fitting parameter. Fig. 9 shows the input map, together with the simulated lifetime map and the experimental PL-image. There is a quite good correspondence between simulated and experimental lifetime maps. Fig. 9 d) compares the simulated and experimental lifetime along the line indicated line in the image c). The ability of simulating the lifetime map after PDG, from an PL image after PDG + firing by only fitting the recombination strength of two types of the GBs indicates that the major effect of a simulated firing process after PDG on commercial material from the central part of the ingot is passivation of the GBs. The firing process has no major impact on recombination in the bulk grains. Also the recombination properties of most of the GB are similar and can be described using the same $\tau_{R.}$

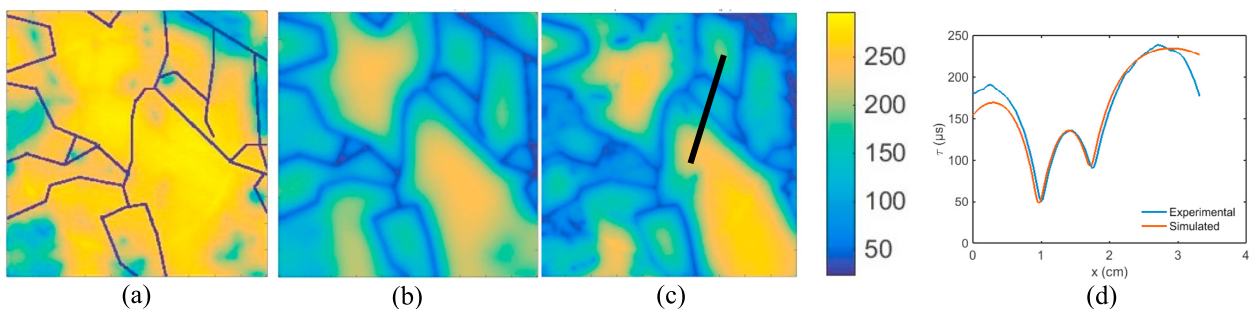

Fig. 9. (a) Bulk lifetime after PDG + firing with two types of GBs indicated.(b) Simulated lifetime map after PDG. (c) Calibrated PL image after PDG (d) Linescan showing the fit between simulated and experimental effective lifetime.

7. Conclusion

Diffusion of charge carriers in double side passivated samples has been simulated in 1D along a line scan, and in 2D for the full wafer surface. For large grains only affected by recombination due to a single grain boundary, the recombination velocity can be calculated from a simple 1D line scan. However, in HPMC-Si most of the grains are small and the carrier concentration is usually affected by recombination at multiple GBs. If more than one GB influences on the carrier concentration 2D modeling of carrier diffusion is required, before the recombination velocity can be found by integrating τ_R over the width of the GB. The bulk lifetime in grains and at GBs τ_R is input as fitting parameters to the simulation. When there is a good correspondence between the simulated map and the measured PL-image, the fitted τ_R of the grains corresponds to the carrier lifetime in bulk unaffected by diffusion off carriers. τ_R at the GB gives a quantitative measure of the recombination strength of the GB. The output of our simulations are similar to what you can achieve by using image de-smearing algorithms to find the bulk lifetime [22]. The bulk lifetime image from our simulations was also compared to the bulk lifetime measured on a neighboring sample after PDG + firing, which turned out to be very similar. The lifetime image after PDG could be well reproduced by using the lifetime after PDG + firing as input to the simulation and fitting the GB recombination velocity. For the samples investigated in this work, the net effect of hydrogen passivation is passivation of the GBs, while there is only minor change in the bulk grains.

Acknowledgements

Funding was provided through the EnergiX programme under project number 228930. Thanks to the Norwegian Research Council and the industry partners; The Quartz Corp AS, Steuler Solar Technology AS, REC Solar and REC Silicon.

References

[1] Coletti G, Sensitivity of state-of-the-art and high efficiency crystalline silicon solar cells to metal impurities, Progress in Photovoltaics: Research and Applications, 2013:21: 1163-1170.
[2] Kveder V, Kittler M, Schröter W, Recombination activity of contaminated dislocations in silicon: A model describing electron-beam-induced current contrast behavior, Physical Review B, 2001:63: 115208.
[3] Schindler F, Michl B, Schon J, et al., Solar Cell Efficiency Losses Due to Impurities From the Crucible in Multicrystalline Silicon, IEEE Journal of Photovoltaics, 2014:4: 122-129.
[4] Buonassisi T, Istratov AA, Peters S, et al., Impact of metal silicide precipitate dissolution during rapid thermal processing of multicrystalline silicon solar cells, Applied Physics Letters, 2005:87: 121918.
[5] Liu AY, Walter D, Phang SP, et al., Investigating Internal Gettering of Iron at Grain Boundaries in Multicrystalline Silicon via Photoluminescence Imaging, IEEE Journal of Photovoltaics, 2012:2: 479-484.
[6] Rinio M, Yodyungyong A, Keipert-Colberg S, et al., Recombination in ingot cast silicon solar cells, physica status solidi (a), 2011:208: 760-768.
[7] Ryningen B, Stokkan G, Kivambe M, et al., Growth of dislocation clusters during directional solidification of multicrystalline silicon ingots, Acta Materialia, 2011:59: 7703-7710.
[8] Stokkan G, Hu Y, Mjøs Ø, et al., Study of evolution of dislocation clusters in high performance multicrystalline silicon, Solar Energy Materials and Solar Cells, 2014:130: 679-685.
[9] Søndenå R, Gjessing J, Angelskår H, et al., Effect of dislocations on the electrical response of mulicrystalline silicon solar cells. , in: 28th European Photovoltaic Solar Energy Conference and Exhibition, Paris, 2013.
[10] Lan CW, Lan WC, Lee TF, et al., Grain control in directional solidification of photovoltaic silicon, Journal of Crystal Growth, 2012:360: 68-75.
[11] Yang YM, Yu A, Hsu B, et al., Development of high-performance multicrystalline silicon for photovoltaic industry, Progress in Photovoltaics: Research and Applications, 2015:23: 340-351.
[12] Wong YT, Hsu C, Lan CW, Development of grain structures of multi-crystalline silicon from randomly orientated seeds in directional solidification, Journal of Crystal Growth, 2014:387: 10-15.
[13] Gindner S, Karzel P, Herzog B, et al., Efficacy of Phosphorus Gettering and Hydrogenation in Multicrystalline Silicon, Photovoltaics, IEEE Journal of, 2014:4: 1063-1070.
[14] Syre M, Karazhanov S, Olaisen BR, et al., Evaluation of possible mechanisms behind P gettering of iron, J. Appl. Phys., 2011:110: -.

[15] Wiig MS, Adamczyk K, Haug H, et al., The Effect of Phosphorus Diffusion Gettering on Recombination at Grain Boundaries in HPMC-Silicon Wafers, Energy Procedia, 2016:92: 886-895.
[16] Takahashi I, Usami N, Mizuseki H, et al., Impact of type of crystal defects in multicrystalline Si on electrical properties and interaction with impurities, J. Appl. Phys., 2011:109: 033504.
[17] Geerligs LJ, Komatsu Y, Rover I, et al., Precipitates and hydrogen passivation at crystal defects in n- and p-type multicrystalline silicon, J. Appl. Phys., 2007:102: 093702-093702-093709.
[18] Sio HC, Trupke T, Macdonald D, Quantifying carrier recombination at grain boundaries in multicrystalline silicon wafers through photoluminescence imaging, J. Appl. Phys., 2014:116: 244905.
[19] Trupke T, Bardos RA, Schubert MC, et al., Photoluminescence imaging of silicon wafers, Applied Physics Letters, 2006:89: 044107.
[20] Mitchell B, Trupke T, Weber JW, et al., Bulk minority carrier lifetimes and doping of silicon bricks from photoluminescence intensity ratios, J. Appl. Phys., 2011:109: 083111.
[21] Phang SP, Sio HC, Macdonald D, Carrier de-smearing of photoluminescence images on silicon wafers using the continuity equation, Applied Physics Letters, 2013:103: -.
[22] Phang SP, Sio HC, Macdonald D, Applications of carrier de-smearing of photoluminescence images on silicon wafers, Progress in Photovoltaics: Research and Applications, 2016:24: 1547-1553.
[23] Liu AY, Sun C, Markevich VP, et al., Gettering of interstitial iron in silicon by plasma-enhanced chemical vapour deposited silicon nitride films, J. Appl. Phys., 2016:120: 193103.